



Dear Author

Here are the proofs of your article.

- You can submit your corrections **online**, via **e-mail** or by **fax**.
- For **online** submission please insert your corrections in the online correction form. Always indicate the line number to which the correction refers.
- You can also insert your corrections in the proof PDF and **email** the annotated PDF.
- For **fax** submission, please ensure that your corrections are clearly legible. Use a fine black pen and write the correction in the margin, not too close to the edge of the page.
- Remember to note the **journal title**, **article number**, and **your name** when sending your response via e-mail or fax.
- **Check** the metadata sheet to make sure that the header information, especially author names and the corresponding affiliations are correctly shown.
- **Check** the questions that may have arisen during copy editing and insert your answers/corrections.
- **Check** that the text is complete and that all figures, tables and their legends are included. Also check the accuracy of special characters, equations, and electronic supplementary material if applicable. If necessary refer to the *Edited manuscript*.
- The publication of inaccurate data such as dosages and units can have serious consequences. Please take particular care that all such details are correct.
- Please **do not** make changes that involve only matters of style. We have generally introduced forms that follow the journal's style.
- Substantial changes in content, e.g., new results, corrected values, title and authorship are not allowed without the approval of the responsible editor. In such a case, please contact the Editorial Office and return his/her consent together with the proof.
- If we do not receive your corrections **within 48 hours**, we will send you a reminder.
- Your article will be published **Online First** approximately one week after receipt of your corrected proofs. This is the **official first publication** citable with the DOI. **Further changes are, therefore, not possible.**
- The **printed version** will follow in a forthcoming issue.

Please note

After online publication, subscribers (personal/institutional) to this journal will have access to the complete article via the DOI using the URL:

<http://dx.doi.org/10.1007/s10544-014-9864-2>

If you would like to know when your article has been published online, take advantage of our free alert service. For registration and further information, go to:

<http://www.link.springer.com>.

Due to the electronic nature of the procedure, the manuscript and the original figures will only be returned to you on special request. When you return your corrections, please inform us, if you would like to have these documents returned.

Metadata of the article that will be visualized in OnlineFirst

Please note: Images will appear in color online but will be printed in black and white.

1	Article Title	Rapid prototyping of multi-scale biomedical microdevices by combining additive manufacturing technologies
2	Article Sub- Title	
3	Article Copyright - Year	Springer Science+Business Media New York 2014 (This will be the copyright line in the final PDF)
4	Journal Name	Biomedical Microdevices
5	Family Name	Lantada
6	Particle	
7	Given Name	Andrés Díaz
8	Suffix	
9	Corresponding Author	Organization Universidad Politécnica de Madrid (UPM)
10		Division Product Development Laboratory, Mechanical Engineering & Manufacturing Department
11		Address José Gutiérrez Abascal, Madrid 28006, Spain
12		e-mail adiaz@etsii.upm.es
13	Family Name	Hengsbach
14	Particle	
15	Given Name	Stefan
16	Suffix	
17	Author	Organization Institute of Microstructure Technology, Karlsruhe Institute of Technology (KIT)
18		Division
19		Address Hermann-von-Helmholtz-Platz 1, Eggenstein-Leopoldshafen 76344, Germany
20		e-mail
21		Received
22	Schedule	Revised
23		Accepted
24	Abstract	The possibility of designing and manufacturing biomedical microdevices with multiple length-scale geometries can help to promote special interactions both with their environment and with surrounding biological systems. These interactions aim to enhance biocompatibility and overall performance by using biomimetic approaches. In this paper, we present a design and manufacturing

procedure for obtaining multi-scale biomedical microsystems based on the combination of two additive manufacturing processes: a conventional laser writer to manufacture the overall device structure, and a direct-laser writer based on two-photon polymerization to yield finer details. The process excels for its versatility, accuracy and manufacturing speed and allows for the manufacture of microsystems and implants with overall sizes up to several millimeters and with details down to sub-micrometric structures. As an application example we have focused on manufacturing a biomedical microsystem to analyze the impact of microtextured surfaces on cell motility. This process yielded a relevant increase in precision and manufacturing speed when compared with more conventional rapid prototyping procedures.

-
- | | | |
|----|-----------------------------|---|
| 25 | Keywords separated by ' - ' | Fractals - Surface topography - Material texture - Materials design - Computer-aided design - Additive manufacturing - Direct laser writing |
|----|-----------------------------|---|
-
- | | | |
|----|-----------------------|--|
| 26 | Foot note information | |
|----|-----------------------|--|

Rapid prototyping of multi-scale biomedical microdevices by combining additive manufacturing technologies

Stefan Hengsbach · Andrés Díaz Lantada

Abstract The possibility of designing and manufacturing biomedical microdevices with multiple length-scale geometries can help to promote special interactions both with their environment and with surrounding biological systems. These interactions aim to enhance biocompatibility and overall performance by using biomimetic approaches. In this paper, we present a design and manufacturing procedure for obtaining multi-scale biomedical microsystems based on the combination of two additive manufacturing processes: a conventional laser writer to manufacture the overall device structure, and a direct-laser writer based on two-photon polymerization to yield finer details. The process excels for its versatility, accuracy and manufacturing speed and allows for the manufacture of microsystems and implants with overall sizes up to several millimeters and with details down to sub-micrometric structures. As an application example we have focused on manufacturing a biomedical microsystem to analyze the impact of microtextured surfaces on cell motility. This process yielded a relevant increase in precision and manufacturing speed when compared with more conventional rapid prototyping procedures.

Keywords Fractals · Surface topography · Material texture · Materials design · Computer-aided design · Additive manufacturing · Direct laser writing

S. Hengsbach
Institute of Microstructure Technology, Karlsruhe Institute of Technology (KIT), Hermann-von-Helmholtz-Platz 1, 76344 Eggenstein-Leopoldshafen, Germany

A. D. Lantada (✉)
Product Development Laboratory, Mechanical Engineering & Manufacturing Department, Universidad Politécnica de Madrid (UPM), José Gutiérrez Abascal, 28006 Madrid, Spain
e-mail: adiaz@etsii.upm.es

1 Introduction

36

Biomedical devices that include geometries and functions on multiple length scales and at different locations are able to interact with their environment and surrounding living systems in a more controlled and accurate way. Multi-scale biomedical devices help to promote biomimetic approaches, as living organisms also exhibit forms and functions at different scales (Place et al. 2009), thus helping to improve aspects such as biocompatibility and overall performance. Therefore, progressive research into design and manufacturing strategies that promote hierarchical materials and structures and their integration into complex appliances is helping to improve both the diagnostic and therapeutic results of several biodevices. In biomedical sciences, fields such as prosthetics (Ponche et al. 2010; Anselme et al. 2010), health-monitoring and diagnosis (Reljin & Reljin 2002), tissue engineering (Hosseinkhani et al. 2010; Hosseinkhani et al. 2007) and even biofabrication (Borchers et al. 2012) are already starting to take advantage of multi-scale approaches, the applications of which are continuously evolving.

Directly related to the concept of multi-scale geometries, material surface topography has an extraordinary influence on several relevant properties linked to final material (and device) performance. These properties include friction coefficient (Archard 1974), wear resistance (Bushan et al. 1995), self-cleaning ability (Barthlott & Neinhuis 1997), biocompatibility (Buxboim & Discher 2010), optical response (Berginski et al. 2007), touch perception, overall aesthetic aspect and even flavor (Briones et al. 2006), to cite just a few. Thus, topography also plays a determinant role in material selection in engineering design, especially in the field of micro and nanosystem development for biomedical engineering, where the effects of topography on the incorporation of advanced properties are even more remarkable.

37
38
39
40
41
42
43
44
45
46
47
48
49
50
51
52
53
54
55
56
57
58
59
60
61
62
63
64
65
66
67
68
69
70

71 Normally, material surface topography is a consequence of
 72 a material's natural state. It can also be the result of machining
 73 processes, chemical attacks or post-processes used to manu-
 74 facture a device or product. Several strategies for modifying
 75 material topographies and surface properties (towards hierar-
 76 chical materials, structures and multi-scale devices) have tak-
 77 en advantage of conventional surface micromachining
 78 (Madou 2002), laser ablation (Chandra et al. 2010),
 79 micromolding (Martin & Aksay 2005), biomimetic
 80 templating (Pulsifier & Lakhtakia 2011), physical and chem-
 81 ical vapor deposition processes (Kwasny 2009), sol-gel pro-
 82 cedures (Jedlicka et al. 2007) and molecular self-assembly
 83 (Rahmawan et al. 2013). All these processes require enormous
 84 hands-on expertise and the final result depends on several
 85 control parameters whose interdependencies are normally
 86 complex to understand, characterize, model and master
 87 (Gad-el-Hak 2003). As can be seen from the previously cited
 88 documents, top-down and bottom-up approaches for
 89 controlling surface properties co-exist and in many cases
 90 complement each other (Naik et al. 2009). The former
 91 are more focused on mass-production (as they are de-
 92 rived from the microelectronic industry), while the latter
 93 provide remarkable geometric versatility.

94 Combinations of top-down and bottom-up approaches are
 95 frequent and have usually focused on manufacturing the larger
 96 micrometric features by means of top-down processes
 97 (micromachining, etching, etc.). The smaller nanometric de-
 98 tails, such as for the rapid prototyping of patterned functional
 99 nanostructures (Fan et al. 2000), are made using bottom-up
 100 techniques (like CVD, PVD, sol-gel, self-assembly, ink-jet
 101 printing). Normally these combinations are not aimed at
 102 obtaining 3D features at different scales, but at incorporating
 103 some surface patterns, 2D 1/2 geometries or some sort of
 104 physical-chemical functionality, such as enhancing bio-
 105 compatibility and implementing special actuating-sensing
 106 functions.

107 Currently, advances in computer-aided design and in high-
 108 precision additive manufacturing technologies based on layer-
 109 by-layer deposition or construction are opening new horizons
 110 for controlling surface topography. They are being used from
 111 the design stage and can be applied in a manner that is very
 112 direct, rapid and simple. This is enabling the prototyping of
 113 multi-scale designs and hierarchical structures. Even though
 114 conventional computer-aided design packages are only capa-
 115 ble of handling Euclidean geometries and mainly rely on
 116 simple operations (sketch based operations, extrusions, pads,
 117 holes, circular grooves, etc.) for obtaining "soft" solids and
 118 surfaces, recent approaches relying on the use of matrix-based
 119 programming have already proved to be useful for designing
 120 rough surfaces and textured objects adequately described by
 121 fractal geometries (Mandelbrot 1982a; Falconer 2003a). In
 122 parallel, the continued progress in additive manufacturing
 123 technologies (also called "solid free-form fabrication" due to

the complex geometries attainable), especially during the last
 decade, has increased the range of materials capable of being
 additively processed and greatly promoted their precision,
 even down to nanometric features. This has implications in
 the development of advanced materials and metamaterials,
 many of which benefit from multi-scale approaches
 (Bückmann et al. 2012; Röhrig et al. 2012).

Ultra-high precision additive manufacturing technologies,
 however, mainly direct-laser writing based on two-photon
 polymerization, despite being capable of yielding nanometric
 details, are very slow and the attainable devices are normally
 smaller than 1 mm³. Such tiny devices are normally aimed at
 very specific studies (i.e. single-cell mechanical-biological
 experiments). Obtaining successful implants, as well as
 easy-to-handle microsystems, is still challenging since most
 biodevices and medical appliances, either for diagnostic or for
 therapeutic tasks, are at least several mm³. On the other hand,
 industrial rapid prototyping (i.e. laser stereolithography,
 digital-light processing and selective laser sintering), in spite
 of being fast and capable of yielding larger devices, is limited
 to manufacturing precisions typically in the 50–250 μm range.
 It is thus still unable to produce biomedical microdevices with
 ad hoc features for interacting at the molecular or even cellular
 level.

In this paper, we present a design and manufacturing pro-
 cedure for obtaining multi-scale biomedical microsystems that
 is based on the combination of two additive manufacturing
 processes: a conventional laser writer to manufacture the
 overall device structure, and a direct-laser writer based on
 two-photon polymerization to yield the smallest details. The
 process stands out for its versatility, accuracy and manufactur-
 ing speed and allows for the manufacture of microsystems and
 implants with overall sizes up to several millimeters and with
 details down to sub-micrometric structures. The following
 section explains the methods and materials used. We then
 present our main results, propose some future directions and
 detail our concluding remarks.

2 Materials and methods

2.1 Design process

As application example we have selected a biomedical
 microsystem aimed at addressing the influence of
 microtextures on cell motility. The system includes two
 microchambers connected by several microchannels to guide
 cell movement, each with a different texture at its bottom. The
 cell motility experiment should begin adding cells to one of
 the chambers and growth factors to the other one, so as to
 promote cell movement from one chamber to another.

The design presented here is inspired by existing devices
 (Díaz 2013), though it has been adapted to scales better suited

173 to interacting at a cellular level. Previous designs and proto-
 174 types included 300- μm wide and 3-mm long channels and
 175 were manufactured using conventional digital light process-
 176 ing. Figure 1 shows the matrix-based design (see description
 177 below) of microtextured channels, with the aforementioned
 178 preliminary rapid prototype obtained by digital light process-
 179 ing, and cell culture results that exhibit adequate attachment of
 180 cells within a textured channel. One of the main limitations of
 181 this preliminary device is that the microchannels are too wide
 182 for adequate assessment of cell motility, since several cells can
 183 enter the channel at once. In addition, the microtextures

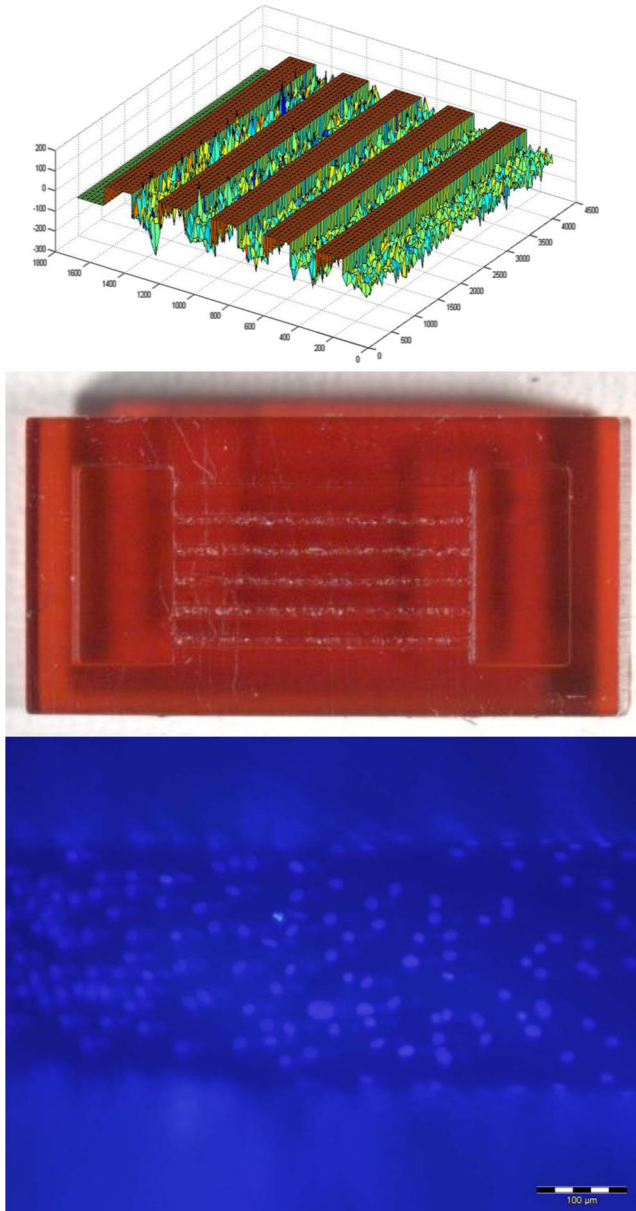
attainable by conventional rapid prototyping have a typical
 height of 50–250 μm , what is not perceived by single cells as a
 real texture.

For more adequate interactions at a cellular level, 30- μm
 wide channels and 1–5 μm high textures, similar to the di-
 mensions of pseudopods and cytoplasmatic deformations,
 would be advisable. At the same time, the overall device size
 cannot be importantly reduced if it is to remain manipulable.
 Fulfilling both requirements suggests a multi-scale approach,
 as we will attempt to explain further on. This approach uses
 one technology and related material to manufacture the overall
 structure, and another technology and related material for the
 smallest details.

The design process, then, also includes combinations of
 different processes. First, the overall structure, which mainly
 comprises the different walls of the two circular
 microchambers and the six microchannels, is designed using
 conventional 3D computer-aided design methods. The CAD
 files can be converted into .stl (standard tessellation language)
 format, currently the most common file type used in 3D
 additive manufacturing. Different technologies including as
 digital light processing, conventional laser stereolithography,
 selective laser sintering or melting and fused deposition
 modeling allow .stl file as information input. The specific
 method chosen would depend on the desired material and
 precision (in our case we used a Heidelberg Instruments
 DWL66fs laserwriter). There is also the possibility of
 converting the 3D design into a black-white mask for 2D $\frac{1}{2}$
 manufacture of the overall structure using lithographic ap-
 proaches typical to the electronic industry.

Subsequently, to incorporate the desired high-precision
 microtextures (capable of interacting at a cellular level), addi-
 tional design operations rely on the generation of simple
 geometries via matrix-based approaches. In such matrix-
 based designs the geometries are stored in the form of [X, Y,
 Z (x, y)] matrices, where X and Y are column vectors with the
 x and y components of the working grid, and Z (x, y) is a
 column vector whose components are the height values for
 each (x, y) couple (spherical and cylindrical coordinates can
 be used for the cases of spherical and cylindrical meshes).
 Then, fractal features can be introduced to incorporate con-
 trolled random textures to the initially regular meshes (z_0), as
 previously detailed (Díaz Lantada et al. 2010). In this paper
 we use fractional Brownian surface models (Mandelbrot
 1982b; Falconer 2003b) to incorporate the desired height
 fluctuations by means of the following equation:

$$z(x, y) = z_0 + m \cdot \sum_{k=1}^{\infty} C_k \lambda^{-\alpha k} \cdot \sin(\lambda^k [x \cos(B_k) + y \sin(B_k) + A_k])$$



Q1 Fig 1 Matrix-based design of microtextured channels. Rapid prototype obtained by digital-light processing and results from cell culture, showing adequate attachment of cells within a textured channel. Adapted from: A. Díaz Lantada, Handbook on advanced design and manufacturing technologies for biomedical devices, Springer, 2013

The models use several random functions (A_k, B_k, C_k) and control constants (λ, α, m), and an initial height function “ z_0 ” can also be introduced. It is interesting to note that in fractional

184
185
186
187
188
189
190
191
192
193
194
195
196
197
198
199
200
201
202
203
204
205
206
207
208
209
210
211
212
213
214
215
216
217
218
219
220
221
222
223
224
225
226
227
228
229
230
231
232
233
234

Q2

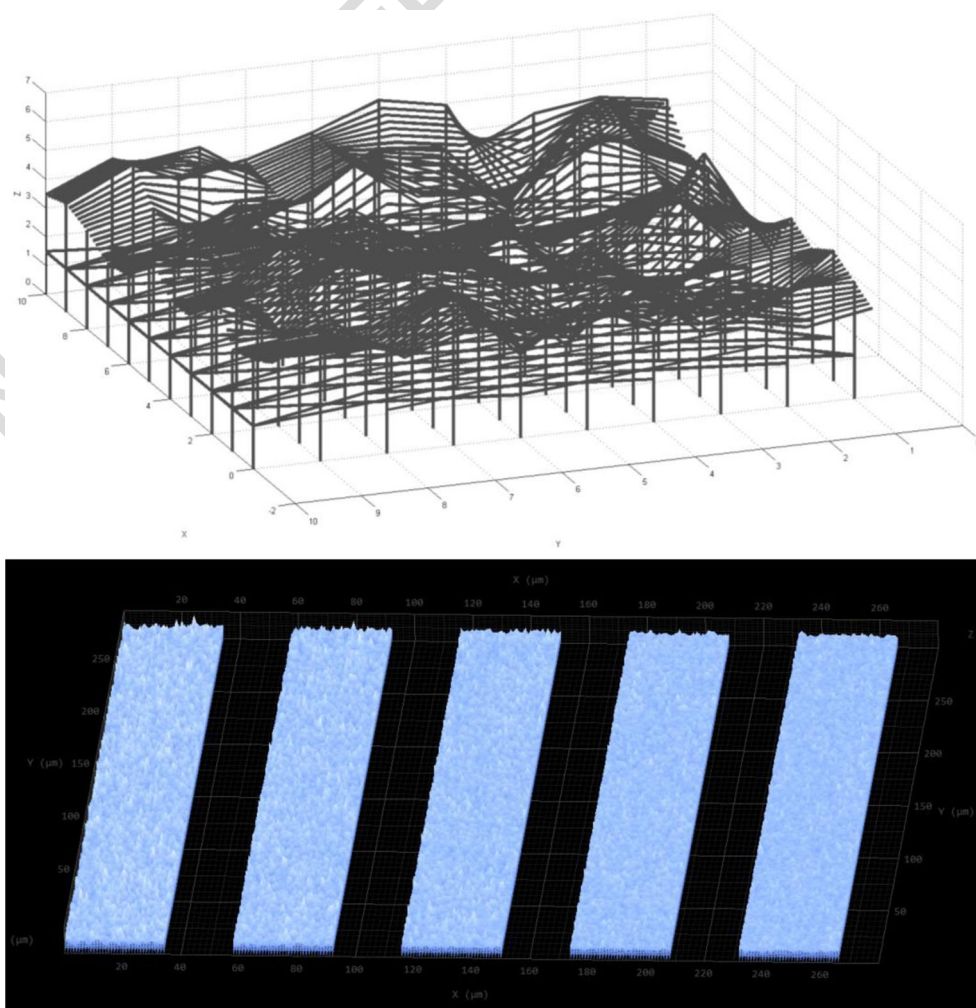
235 Brownian models (Mandelbrot 1982b; Falconer 2003b), the
 236 fractal dimension can be related to the exponent α , where $D=$
 237 $3 - \alpha$, with $0 < \alpha < 1$. Therefore, higher values of “alfa” lead to
 238 more “planar” surfaces or textures and lower values of “alfa”
 239 lead to more “three-dimensional” or spiky surfaces or textures,
 240 as shown in Figs. 1a and 2b. Adequately assessing the most
 241 beneficial values of “alfa” for different applications is still a
 242 matter of research; for instance, our team has addressed its
 243 impact on cell culture (Díaz Lantada et al. 2011). By truncat-
 244 ing the aforementioned sum of infinite terms, basic fractal
 245 geometries can be obtained in matrix form and further con-
 246 verted into recognizable CAD formats, typically .stl (standard
 247 tessellation language) .igs (initial graphics exchange specifi-
 248 cation) or .dxf (drawing exchange format). In our case the
 249 surface generation has been programmed using Matlab (The
 250 Mathworks Inc.). The use of additional “mesh to solid” con-
 251 verters leads to the final solid files, which can be used as
 252 normal CAD parts for further design, simulation, modeling
 253 and computer-aided manufacturing tasks. The process can be
 254 adapted to the surfaces of any computer-aided designed im-
 255 plant and multi-scale designs are possible, normally using

256 conventional Euclidean surfaces for micrometric – milimetric
 257 features. The fractal term would usually be added for the
 258 100 nm – 10 μm range, in order to promote interactions at
 259 cellular level.

260 One problem associated with incorporating micrometric
 261 textures and microstructures to computer-aided designs in-
 262 volves the final file size. For instance, a micrometric grid of
 263 300 \times 300 points with a clearance between points of 1 μm
 264 leads to a .stl file of around 7 MB and to a .dxf file of around
 265 30 MB. For a useful part measuring several mm^3 , the incor-
 266 poration of a micrometric texture can result in file sizes of
 267 several hundred MB or even a few GB, which is currently
 268 very difficult to manage with computer-aided design
 269 resources.

270 The fact is that the “universal” .stl, .igs, .dxf and other
 271 formats are not optimal, especially for fractal-based designs,
 272 which can be described and programmed with just one line of
 273 code. For instance a binary .stl file, similar to those we have
 274 used, has typically an 80 character header (generally ignored,
 275 but which should not begin with the word “solid” because that
 276 will lead most software to assume that it is an ASCII .stl file).

Fig 2 **a** Microtextures as lines supported by pillars, as determined by the manufacturing technology. **b** Overview of the different microtextures designed for the channels in the microsystem



277 Following the header, a 4 byte unsigned integer indicates the
278 number of triangular facets in the file. After that integer, each
279 triangle is described by twelve 32-bit-floating point numbers:
280 three for the normal vector and then three for the Cartesian
281 coordinates of each vertex. In consequence, a vertex common
282 to four triangles of the surface is repeated four times in the .stl
283 structure and such description is not optimal. The convention-
284 al CAD geometrical description of these designs unnecessar-
285 ily increases file size. The shift to an algorithmic, rather than
286 descriptive, geometry is a key factor to promote material
287 properties and structure by design and to the further applica-
288 tion of these knowledge-based materials to product develop-
289 ment (Lipson 2012).

290 Even though CAD resources can be utilized to almost
291 directly convert the surfaces generated into solid .stl files, any
292 subsequent slicing of the geometry (a typical operation of the
293 software used to control layer-by-layer manufacturing ma-
294 chines) leads to very slow and expensive manufacturing pro-
295 cesses. In our case, a microtextured surface created on 30
296 $\times 300 \mu\text{m}^2$ channels in which points on the grid are separated
297 by $1 \mu\text{m}$, once converted into a solid and sliced, leads to a
298 manufacturing time of more than 50 h using direct laser writing.

299 In addition, the resist and direct laser writing process used
300 in this study require a distance between parallel written
301 (polymerized) lines of 250 nm, meaning the initial matrix-
302 based design (Fig. 1a) has to be adapted to the manufacturing
303 process. Using a square grid (for each channel) of 30
304 $\times 300 \mu\text{m}^2$, in which the grid points are separated by $1 \mu\text{m}$,
305 the fractal surfaces are generated again and stored in matrix
306 form. Each matrix is completed, as shown schematically in
307 Fig. 2a, by incorporating additional column vectors that store
308 interpolated paths, separated by 250 nm, between the original
309 vectors separated by $1 \mu\text{m}$. Vertical parallel lines, also sepa-
310 rated by 250 nm, are generated under each fractal path so as to
311 provide a supporting structure for surface construction.

312 The design shown in Fig. 2b can be manufactured in just a
313 couple of hours. This is an increase in production speed of more
314 than one order of magnitude when compared with the initial
315 solid model. Material and laser power consumption are also
316 reduced by a similar rate. The time and material saved can be
317 used to manufacture several prototypes so as to methodically
318 compare the effects of different control parameters, such as
319 fractal dimension, laser power used, pre-polymer employed or
320 post-processing operations. These can include the use of critical
321 point dryers or additional post-curing so as to precisely adjust
322 the prototypes to the final production stage. Additional details
323 regarding the manufacturing process are included below.

324 2.2 Manufacturing process

325 Materials: For the initial stage in which the overall structure of
326 the microdevices is manufactured, we used SU-8 spin coated
327 on a silicon wafer. SU-8 (MicroChem Corp.) is a commonly

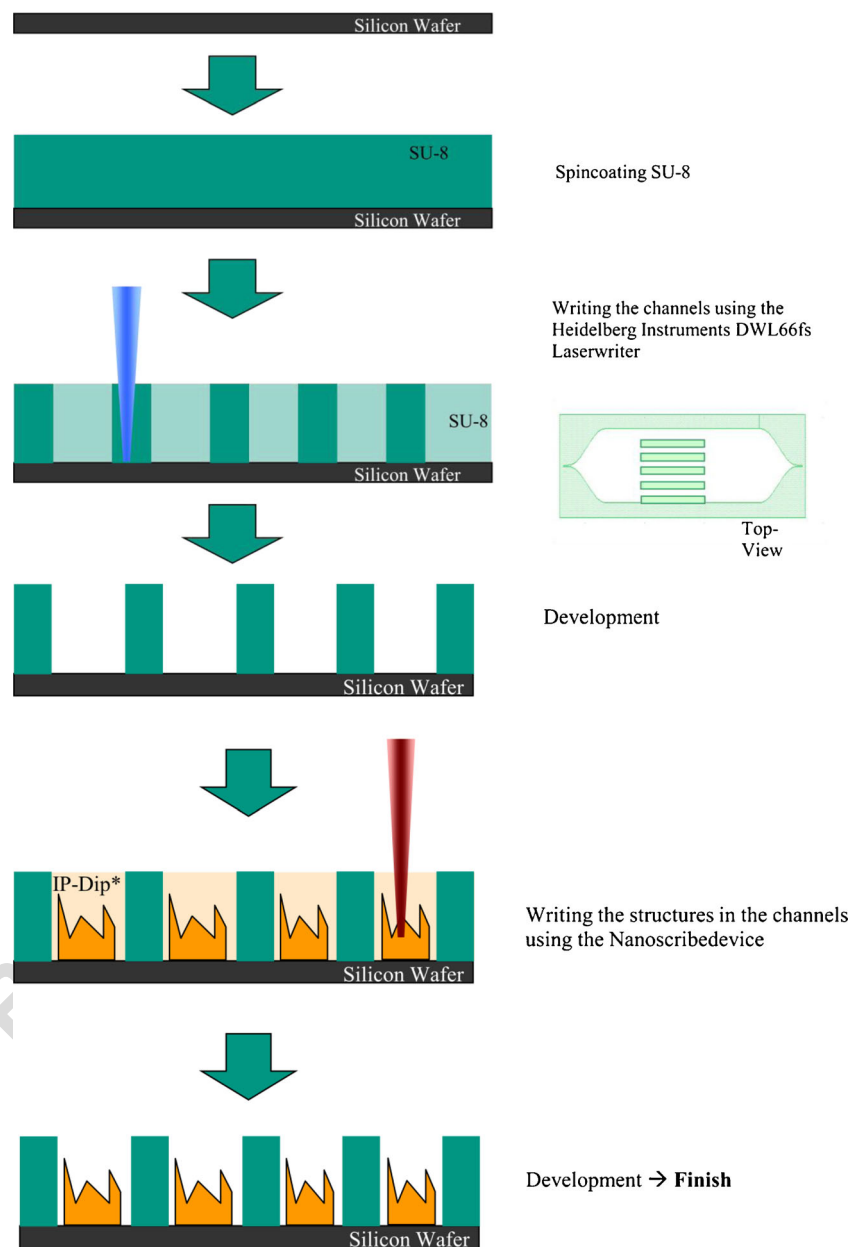
used epoxy-based negative photoresist. It is highly functional, 328
optically transparent and photo imageable to near UV 329
(365 nm) radiation. Cured films or microstructures are very 330
resistant to solvents, acids and bases and have excellent 331
thermal and mechanical stability. They are also important 332
for the promotion of medical applications and studies in 333
the field of tissue repair and engineering (White R. SU-8 334
Photoresist processing: Standard operating procedure. 335
(Online), January, 19 2012). 336

337 For the detailed microtextures within the different chan- 338
nels, a resist with a much lower voxel size than that of the SU- 339
8 is needed. In our case, the resist is also linked to the two- 340
photon polymerization process used. In this study we used the 341
IP-Dip resist (NanoScribe GmbH and related data sheets for 342
additional information), a specially designed photoresist that 343
guarantees ideal focusing and has the highest resolution of any 344
NanoScribe IP-Photoresist (with feature sizes down to 150 nm 345
and minimized shrinkage). This is because its refractive index 346
is matched to the focusing optic (Bückmann et al. 2012).

347 Process: The multi-scale manufacturing process followed 348
is schematically described in Fig. 3 and consists mainly of the 349
following stages. First, a silicon wafer is spin coated with SU- 350
8 and the overall structure of the microsystem is obtained after 351
photopolymerization (using a Heidelberg Instruments 352
DWL66fs laserwriter) and further development. Subsequent- 353
ly, the channels are filled with the IP-Dip photoresist and the 354
microtextures are obtained using the Photonic Professional 355
System from NanoScribe GmbH, the first commercial direct 356
laser writing system based on two-photon polymerization. 357
NanoScribe GmbH (www.nanoscribe.de) was founded in 358
2007 by scientists in the field of photonics as a spin-off com- 359
pany of the Karlsruhe Institute of Technology (www.kit.edu). 360
The company specializes in the innovative technique of 3D 361
laser lithography and produces compact and easy-to-operate 362
table-top laser lithography systems (Photonic Professional). 363
Final super critical drying and development lead to the desired 364
multi-scaled microsystem.

365 The direct laser writing process is noted for its accuracy 366
and versatility, since several resists and even polymer-ceramic 367
mixtures can be manufactured. This process can also be used 368
additively without the need for supporting structures, which 369
allows for the manufacture of especially complex parts with 370
inner details. In short, when focused onto the volume of a 371
photosensitive material, the laser pulses initiate two-photon 372
polymerization via two-photon absorption and subsequent 373
polymerization, normally perceived as a change of resist 374
viscosity. Polymerization only occurs at the focal point, where 375
the intensity of the absorbed light is highest, thus enhancing 376
the accuracy. After illumination of the desired structures inside 377
the resist volume and final development (washing out of the 378
non-illuminated regions) the polymerized material remains in 379
the written 3D form (Ostendorf & Chichkov 2006; 380
Hermatsweiler 2013).

Fig. 3 Schematic depiction of the multi-scale rapid prototyping process



381 It is important to note that the NanoScribe direct laser
 382 writing technology writes the structures differently than
 383 conventional additive or “layer by layer” manufacturing technol-
 384 ogies. In other additive technologies, such as normal laser
 385 stereolithography, selective laser sintering or melting or ink-
 386 jet printing, the manufacturing process starts from a 3D
 387 computer-aided design file, which is sliced into layers with
 388 the help of ad hoc software. Then, the manufacturing is
 389 accomplished layer by layer, by photopolymerization or depo-
 390 sition of material along the boundaries of each layer and
 391 subsequent filling of layers with parallel lines of material. In
 392 the NanoScribe process, the structures are not written layer-
 393 by-layer, but by following three-dimensional paths connected

394 from the beginning to the end of the writing process. This
 395 means that additional programming is usually needed to con-
 396 vert the original CAD files into writable structures, as already
 397 schematized in Fig. 2. In addition, it is important to establish
 398 an adequate writing strategy in order to avoid writing through
 399 already polymerized resist. This can lead to unwanted optical
 400 effects because the polymerized resist has a different refractive
 401 index when compared to the unexposed resist.

402 As mentioned earlier, Matlab (The Mathworks Inc.) is used
 403 to create the structures and also to create the information
 404 exchange files that can be used directly in Nanoscribe Pho-
 405 tonic Professional. The advantage over using more conven-
 406 tional additive-manufacturing slicing software is that the

407 structure can be calculated and optimized based on the writing
408 strategy and taking into account energy and time saving
409 issues. Time can be saved by wiring lines in the correct order.
410 Another advantage is that additional control variables can be
411 used and parameter variation can be easily promoted by
412 writing ad hoc programs. Parameter variation (i.e. distance
413 between lines, structure scales, etc.) is especially useful for
414 systematic research and matrix-based designs are helpful for
415 providing this versatility and freedom of design. Finally, com-
416 plex mathematical variables can be used to create complex
417 structures, in keeping with recent tendencies intended to min-
418 imize .stl file size by resorting to algorithmic approaches
419 (Lipson 2012).

420 The choice of laser power depends on the material being
421 processed and has a direct influence on the attainable voxel
422 (here defined as the minimal building block in additive man-
423 ufacture approaches) size. Lower powers lead to smaller voxel
424 sizes, although to start the polymerization at one point, a
425 minimum threshold has to be overcome. This threshold is
426 the minimum laser power that promotes enough energy den-
427 sity at the focal point to start polymerization. Below that
428 power, the possibility of two photons being absorbed at the
429 focus point is too low. If the density at the focal point is too
430 high, inner explosions in the resist occur. In our case, for the
431 fractal structures a minimal possible laser power of 5.5 mW
432 was chosen to create a very detailed surface. At optimal
433 conditions a line width of 150 nm at an aspect ratio of 3.5
434 can be reached.

435 One of the major problems in lithography involves shrink-
436 ing, which affects the accuracy. There are two types of shrink,
437 one linked to the material being processed and one linked to
438 the structure geometry. The former depends on the contractil-
439 ity of the material being processed, and the latter is related to
440 possible structure contractions and collapse during the manu-
441 facture and subsequent development. There are also possible
442 adhesion effects.

Another limiting factor for some applications is the diffi-
culty indirectly processing metals through direct laser writing.
However, it is important to note that organic photoresists, like
SU-8 (MicroChem Corp.) or the IP-Photoresists (NanoScribe
GmbH), hybrid materials, such as the Ormocere[®] organic-
inorganic hybrid polymer family (Fraunhofer-Gesellschaft e.
V.), and the amorphous semiconductor As₂S₃ are capable of
two-photon polymerization, which provides a wide range of
possibilities. In addition, through CVD/PVD coating process-
es, or just by electroplating, final metallization is possible and
casting processes can also be used for additional versatility.
Moreover, advanced research groups, as well as companies,
are focusing on the continuous development of novel materi-
als, including photoelastomers, photopolymers and polymer-
ceramic composites. These materials, even when used for
medical applications, can be structured by means of direct
laser writing (Ostendorf & Chichkov 2006).

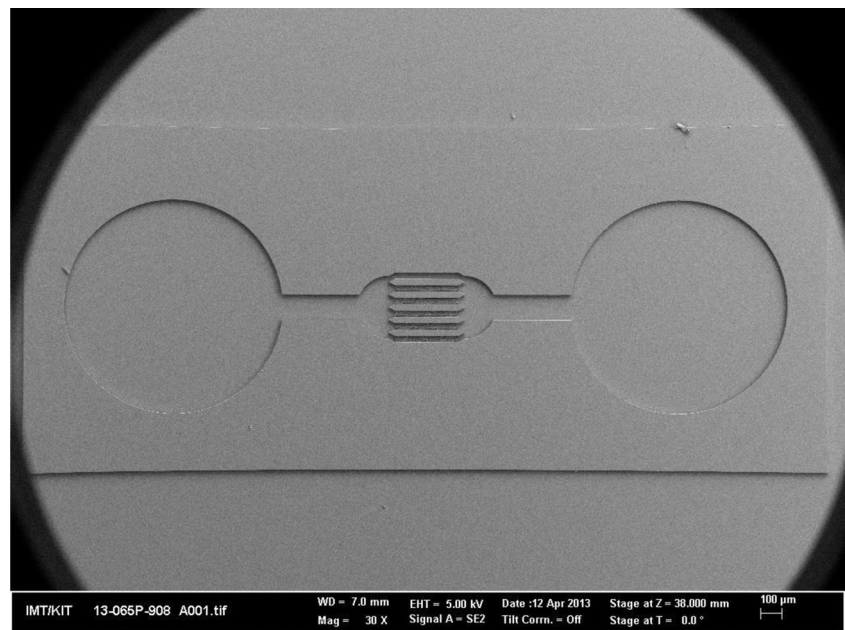
3 Results

Figure 4 shows the final multiscale biomedical microsystem
for assessing the effect of surface texture on cell motility. Its
outer structure (circular chambers and channel walls) was
obtained using the Heidelberg Laser Writer, and the textured
channels were created using the NanoScribe system. Figure 5
shows several details from the different micro-textured chan-
nels obtained via direct-laser writing and helps to highlight the
influence of control parameter “alfa” on surface topography.
This parameter is linked to roughness and fractal dimension.
In short, higher values of “alfa” lead to more planar surfaces
and lower values of “alfa” lead to more spiky surfaces. In our
case we used a different value of “alfa” for each channel so as
to control the textures of the different channels from the design
(Fig. 2b) stage. Figure 5 shows the different values of “alfa”
used: 0.1; 0.3; 0.5; 0.7 & 0.9, with related fractal dimensions
of 2.9; 2.7; 2.5; 2.3 & 2.1. An additional planar (with fractal
dimension equal 2) was also included for use as a control
channel in forthcoming *in vitro* trials.

The detailed images included in Figs. 5 and 6a help to show
the accuracy of the micro-texturing process. The similarity
between the initial design and the final prototype validates the
proposed approach for controlling surface topography in
microsystems. It is interesting to note that the typical “steps”
that can be seen in several additive manufactured devices
when using more conventional technologies, cannot be appre-
ciated here. This is because the NanoScribe process does not
work using a sliced CAD file, but by writing lines in three-
dimensional space (in a similar way as schematically depicted
in Fig. 2a). Consequently, the process is additive but not “layer
by layer”: instead of appreciating the different slices and steps,
several lines can be perceived upon the different surfaces,
according to the different paths followed by the laser. In any
case, for the purpose of the microsystem, these lines do not
affect the functionality as much as the layered and stepped
geometries usually obtained by other high-precision rapid
prototyping technologies, including digital-light processing
and micro-stereolithography.

The detailed image in Fig. 6b shows the fractal
surface and supporting pillars obtained by two-photon
polymerization of the previously rapid manufactured
microsystem structure of channels and chambers, which
shows the benefits of combining processes and materials
towards multi-scale microsystems. Some shrinking dur-
ing the critical drying process (around 4 %) is present
and has led to some de-attachment between the
microtextured surfaces and the channel walls. This
shrinking can be reduced to values of around 1-2 %
by incorporating some additional outer pillars connected
to the surface. These pillars act as support structures
and absorb stress, as previous research has shown
(Norman et al. 2013).

Fig. 4 Overview of the multiscale biomedical microsystem, with the outer structure obtained using the Heidelberg Laser Writer and with the textured channels obtained using the NanoScribe system



Besides, the detailed view helps to verify that the microtextured surfaces are adequately supported by the structure of pillars, which do not penetrate through the surface due to adequate photopolymerization. Lower laser powers lead to lower degrees of polymerization and to the collapse of fractal surfaces, as happened in some of our preliminary manufacturing tests. On the other hand, increased laser power can promote multi-photon, instead of two-photon, absorption. This results in lower accuracy and in an uncontrolled response of the resist during polymerization, normally leading to significant defects. The process must thus be adequately adjusted so as to reach the adequate polymerization level.

Some design improvements, such as the incorporation of a progressive ramp at the beginning of each channel to help the cells crawl on the microtextured surfaces supported by pillars and enter the different channels, as well as the inclusion of

some additional micro-gripping structures at the edge of the microsystem to simplify its handling, can enhance the final functionality. Regarding manufacturing, improvements in the final critical drying process can also help to reduce residual stresses, hence minimizing shrinkage of the IP-Dip photoresist and preventing de-attachments. In spite of these possible improvements, it is important to note that the writing speed for the direct laser writing part of the process can be increased by more than one order of magnitude by using a surface design supported by pillars, when compared with a solid design. The quantity of resist used and the laser power consumed are similarly reduced, hence resulting in a remarkably low-cost and sustainable solution.

The surfaces and prototypes obtained can be used as final parts, they can be have additional coatings or functionalities, i.e. for micromolding (Norman et al. 2013), and they can be

Fig. 5 Close-up of the different micro-textured channels obtained via direct-laser writing. Influence of control parameter “alfa” on surface topography, related to roughness and fractal dimension

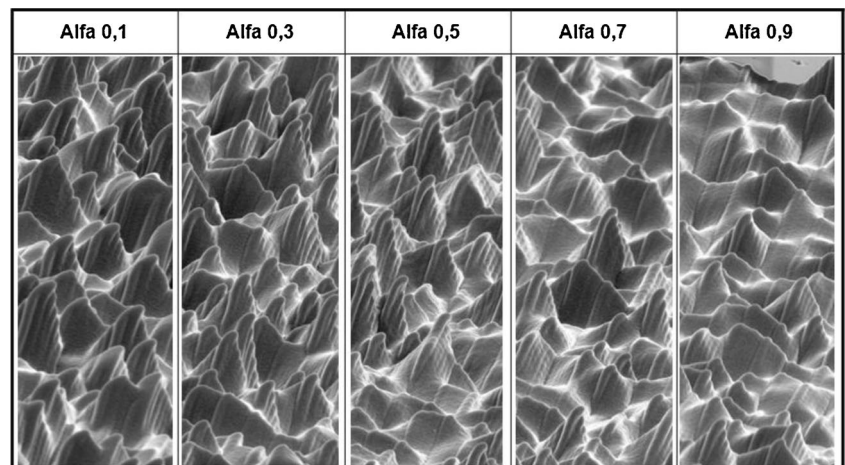
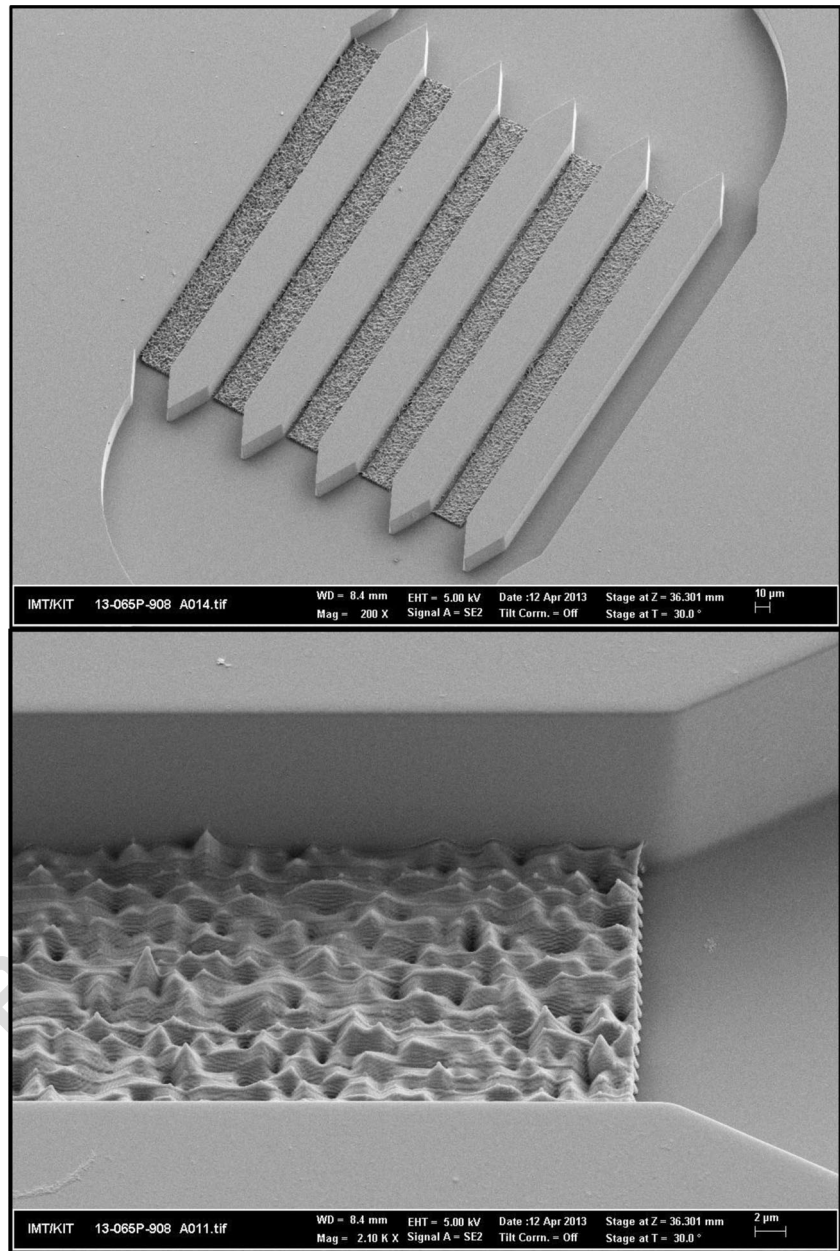


Fig. 6 Close-up of the different micro-textured channels (upper image) Close-up of the fractal surface and supporting pillars obtained by two-photon polymerization of the previously rapid manufactured microsystem structure of channels and chambers (lower image)



used as green parts for obtaining replicas in other materials, depending on the application. For instance, following metallic chemical- or physical-vapor deposition to enhance surface conductivity, the surfaces can be electroplated with nickel and further used as inserts for injection molding of thermoplastics or of ceramic powders with bonding agents before final sintering. PDMS molds can be also directly obtained by casting upon the surfaces and used as rapid molds for casting several polymers. Interesting functionalizations for further integration with electronics (Simon et al. 2013) may also open new horizons. These combinations of prototyping and mass-production processes will help to increase the range of applications of these micro-textured surfaces, providing a wider

palette of materials whose surface topography can be precisely controlled from the design stage.

Future trials will focus on assessing the possibilities of the designed and manufactured microsystems by culturing real cells on them. The material is adequate for cell culture and the manufacturing precision allows for real interaction at the cellular level, as previous ground-breaking research has shown (Klein et al. 2010). However, we still need to improve some capabilities and resources from our labs involving micromanipulation facilities, cell culture related equipment and the cells themselves, in preparation for these trials. In any case the device has the potential to address cell motility and the influence of surface topography on the cells, with roughness

in the range of 1–5 μm , which is much more adequate than the 200–350 μm from the original proof-of-concept from Fig. 1 (Díaz 2013). The channel width of 30 μm is aimed at preventing several cells from crawling in parallel and at promoting single-cell tracking, which could not be obtained with our previous device (Díaz 2013). The capabilities of these microsystems can be complemented by the use of other fractal features that affect cell dynamics, behavior and differentiation into relevant tissues (Díaz Lantada et al. 2013).

Finally we would like to emphasize the level of accuracy achieved and the quality of the microsystem obtained, even when considering the aforementioned minor defects inherently related to the multi-scale process utilized. The channels obtained have a length of 300 μm and a width of 30 μm , which will prevent several cells from entering a channel at once and allow for single cell tracking. It will also enhance the motility monitoring process in future *in vitro* trials. In addition, the fractal microtextures obtained are in the initially desired range of 1–5 μm , thus having the same order of magnitude as cytoskeleton deformations and allowing for a more adequate interaction at a cellular level. Future trials will allow us to assess the actual impact of fractal dimension on cell motility. In an effort to promote the use of biomimetic approaches or as a complement to recent biomimetic proposals in the field of cancer cell migration (Huang et al. 2013), similar approaches could potentially be used to control the textures of several microsystems and implants.

4 Conclusions

We have presented an enhanced design and manufacturing process for obtaining multi-scale biomedical microdevices that is based on the combination of two additive manufacturing processes: a conventional laser writer to manufacture the overall device structure; and a direct-laser writer based on two-photon polymerization to yield the smallest details. The process excels for its versatility, accuracy and manufacturing speed and allows for the manufacture of microsystems and implants with overall sizes up to several millimeters and with details down to sub-micrometric structures. As an application example we have focused on manufacturing a biomedical microsystem to analyze the impact of microtextured surfaces on cell motility. This process yielded a relevant increase in precision and manufacturing speed when compared with more conventional rapid prototyping procedures.

Regarding future studies, we consider it important to focus on exploring in depth the possible applications of design-controlled multi-scale biomedical microdevices, especially in areas such as cell mechanobiology and multi-scale integration across organic and inorganic interfaces for several types of implantable (either active or passive) medical devices. In addition, we believe it relevant to address further

combinations of micro-nanomanufacturing technologies. This includes the possibility of complementing the procedures detailed herein with other mass-replication technologies, including micro-injection molding and hot-embossing.

We foresee relevant implications of the processes described in areas such as: tribology, due to the potential promotion of adhesion using fractal textures; microfluidics, due to the possibility of controlling the hydrophobicity and hydrophilicity of surfaces by acting on their topography; optics, due to the option of changing surface reflection properties and overall aesthetics; and biomedical engineering, for the promotion of biomimetic designs. Currently we are working to improve the versatility of the design process by allowing for the introduction of controlled texture gradients and different kinds of texture variations within the surfaces of interest.

Acknowledgements This work was carried out with the support of the European Community. We appreciate the support of the European Research Infrastructure EUMINAFab (funded under the FP7 specific programme Capacities, Grant Agreement Number 226460) and its partner, the Karlsruhe Institute of Technology. We are also grateful to Dr. Dieter Maas and to Dr. Thomas Schaller for their kind help and for their support of the EUMINAFab 1140 proposal. We acknowledge reviewers for their positive opinions, encouraging comments and proposals for improvement, which have helped to enhance paper quality, readability, content and final result.

References

- E.S. Place, N. Evans, M. Stevens, Complexity in biomaterials for tissue engineering. *Nat. Mater.* **8**, 457–469 (2009)
- A. Ponche, M. Bigerelle, K. Anselme, Relative influence of surface topography and surface chemistry on cell response to bone implant materials. Part 1: Physico-chemical effects. *Proc. IME. J. Eng. Med.* **224**(12), 1471–1486 (2010)
- K. Anselme, A. Ponche, M. Bigerelle, Relative influence of surface topography and surface chemistry on cell response to bone implant materials. Part 2: Biological aspects. *Proc. IME. J. Eng. Med.* **224**(12), 1487–1507 (2010)
- I.S. Reljin, B.D. Reljin, Fractal geometry and multifractals in analyzing and processing medical data and images. *Arch. Oncol.* **10**(4), 283–293 (2002)
- H. Hosseinkhani, M. Hosseinkhani, S. Hattori, R. Matsuoka, N. Kawaguchi, Micro and nano-scale *in vitro* 3D culture system for cardiac stem cells. *J. Biomed. Mater. Res. A* **94**(1), 1–8 (2010)
- H. Hosseinkhani, M. Hosseinkhani, F. Tian, H. Kobayashi, Y. Tabata, Bone regeneration on a collagen sponge self-assembled peptide-amphiphile nanofiber hybrid scaffold. *Tissue Eng.* **13**(1), 11–19 (2007)
- Borchers K, Bierwisch C, Cousteau J, Engelhard S, Graf C, Jaeger R, Klechowicz N, Kluger P, Krueger H, Meyer W, Novosel E, Refle O, Schuh C, Seiler N, Tovar G, Wegener M, Ziegler T. New cytocompatible materials for additive manufacturing of bio-inspired blood vessels systems. *International Conference on Biofabrication* 2012.
- J. Archard, Surface topography and tribology. *Tribology* **7**(5), 213–220 (1974)
- B. Bushan, J. Israelachvili, U. Landman, Nanotribology: friction, wear and lubrication at the atomic scale. *Nature* **374**, 607–616 (1995)

- W. Barthlott, C. Neinhuis, Purity of the sacred lotus, or escape from contamination in biological surfaces. *Planta* **202**, 1–8 (1997)
- A. Buxboim, D.E. Discher, Stem cells feel the difference. *Nat. Methods* **7**(9), 695–697 (2010)
- M. Berginski, J. Hüpkens, M. Schulte, G. Schöpe, H. Stiebig, B. Rech, The effect of front ZnO:Al surface texture and optical transparency on efficient light trapping in silicon thin-film solar cells. *J. Appl. Phys.* **101**, 074903 (2007)
- V. Briones, J.M. Aguilera, C. Brown, The effect of surface topography on color and gloss of chocolate samples. *J. Food Eng.* **77**(4), 776–783 (2006)
- M.J. Madou, *Fundamentals of microfabrication: The Science of miniaturization*, 2nd edn. (CRC Press, New York, 2002)
- Chandra P, Lai K, Sunj HJ, Murthy NS, Kohn J. UV laser-ablated surface textures as potential regulator of cellular response. *Biointerphases*, **5** (2), 53–59, (2010)
- C.R. Martin, I.A. Aksay, Microchannel molding: A soft lithography-inspired approach to micrometer-scale patterning. *J. Mater. Res.* **20**(8), 1995–2003 (2005)
- D.P. Pulsifier, A. Lakhtakia, Background and survey of bioreplication techniques. *Bioinspir. Biomim* **6**(3), 031001 (2011)
- W. Kwasny, Predicting properties of PVD and CVD coatings based on fractal quantities describing their surface. *J. Achiev. Mater. Manuf. Eng* **37**(2), 125–192 (2009)
- S.S. Jedlicka, J.L. McKenzie, S.L. Leavesley, K.M. Little, T.J. Webster, J.P. Robinson, D.E. Nivens, J.L. Rickus, Sol–gel derived materials as substrates for neuronal differentiation: effects of surface features and protein conformation. *J. Mater. Chem.* **16**(31), 3221–3230 (2007)
- Y. Rahmawan, L. Xu, S. Yang, Self-assembly of nanostructures towards transparent, superhydrophobic surfaces. *J. Mater. Chem. A* **1**(9), 2955–2969 (2013)
- M. Gad-el-Hak, *The MEMS Handbook* (CRC Press, New York, 2003)
- V.M. Naik, R. Mukherjee, A. Majumder, A. Sharma, Super functional materials: Creation and control of wettability, adhesion and optical effects by meso-texturing of surfaces. *Curr. Trends. Sci.* (129–148) (2009). Platinum Jubilee Special
- H. Fan, Y. Lu, A. Stump, S.T. Reed, T. Baer, R. Schunk, V. Perez-Luna, G.P. López, J. Brinker, *Nature* **405**, 56–60 (2000)
- B. Mandelbrot, *The Fractal Geometry of Nature* (W.H. Freeman, San Francisco, 1982a)
- Falconer K. *Fractal Geometry: Mathematical Foundations and Applications*. *John Wiley & Sons Ltd.*, 2003.
- T. Bückmann, N. Stenger, M. Kadic, J. Kaschke, A. Frölich, T. Kennerknecht, C. Eberl, M. Thiel, M. Wegener, Tailored 3D mechanical metamaterials made by dip-in direct-laser-writing optical lithography. *Adv. Mater.* **24**, 2710–2714 (2012)
- M. Röhrig, M. Thiel, M. Worgull, H. Hölscher, Hierarchical structures: 3D direct laser writing of nano-microstructured hierarchical gecko-mimicking surface. *Small* **8**(19), 3009–3015 (2012)
- Díaz Lantada A. *Handbook on advanced design and manufacturing technologies for biomedical devices*. *Springer*, 2013
- A. Díaz Lantada, J.L. Endrino, A.A. Mosquera, P. Lafont, Design and rapid prototyping of DLC coated fractal surfaces for tissue engineering applications. *J. Phys. Conf. Ser.* **252**(1), 012003 (2010)
- B. Mandelbrot, *The Fractal Geometry of Nature* (W.H. Freeman, San Francisco, 1982b)
- Falconer K. *Fractal Geometry: Mathematical Foundations and Applications*. *John Wiley & Sons Ltd.*, 2003.
- A. Díaz Lantada, J. Endrino, V. Sánchez-Vaquero, A.A. Mosquera, P. Lafont Morgado, J.P. García Ruíz, Tissue engineering using novel DLC-coated rapid prototyped scaffolds. *Plasma. Processes. Polym.* **9**(1), 98–107 (2011)
- H. Lipson, Frontiers in additive manufacturing, the shape of things to come. *The Bridge* **42**(1), 5–12 (2012)
- White R. SU-8 Photoresist processing: Standard operating procedure. (Online), January, 19, 2012.
- A. Ostendorf, B.N. Chichkov, Two-photon polymerization: A new approach to micromachining. *Photonics. Spectr.* (October) (2006)
- M. Hermatsweiler, Laserlithografie als Innovationstreiber für Schlüsseltechnologien. *Laser. Technik. J.* (September) (2013)
- J.J. Norman, S.O. Choi, N.T. Tong, A.R. Aiyar, S.R. Patel, M.R. Prausnitz, M.G. Allen, Hollow microneedles for intradermal injection fabricated by sacrificial micromolding and selective electrodeposition. *Biomed. Microdevices* **15**(2), 203–210 (2013)
- D. Simon, T. Ware, R. Marcotte, B.R. Lund, D.W. Smith, M. Di Prima, R.L. Rennaker, W. Voit, A comparison of polymer substrates for photolithographic processing of flexible bioelectronics. *Biomed. Microdevices* **15**(6), 925–939 (2013)
- F. Klein, T. Striebel, Z. Jiang, C.M. Franz, G. Von Freymann, M. Bastmeyer, Elastic fully three-dimensional microstructure scaffolds for cell force measurements. *Adv. Mater.* **22**, 868–871 (2010)
- A. Díaz Lantada, B. Pareja Sánchez, C. Gómez Murillo, J. Urbieta Sotillo, Fractals in tissue engineering: Towards biomimetic cell-culture matrices, microsystems and microstructured implants. *Expert. Rev. Med. Devices.* **10**(5), 629–648 (2013)
- Huang TQ, Qu X, Liu J, Chen S. 3D printing of biomimetic microstructures for cancer cell migration. *Biomedical Microdevices*, DOI [10.1007/s10544-013-9812-6](https://doi.org/10.1007/s10544-013-9812-6), (Online), October, 29, 2013.

AUTHOR QUERIES

AUTHOR PLEASE ANSWER ALL QUERIES.

- Q1. Figures 1-2 contains poor quality resolution (small & blurry text). Please provide revised figures with higher resolution and make sure that the illustration has the specified aspect and is still informative upon reduction.
- Q2. Please check equation if captured and presented correctly.

UNCORRECTED PROOF